

ELASTIC ANALYSIS OF BURIED STRUCTURES SUBJECT TO THREE-DIMENSIONAL SURFACE LOADING

N. S. M. FERNANDO, J. C. SMALL AND J. P. CARTER

School of Civil and Mining Engineering, The University of Sydney, Sydney, N.S.W. 2006, Australia

SUMMARY

A method is presented which may be used to compute the displacements, strains and moments (both in-plane and transverse) in buried structures such as pipelines and culverts subjected to longitudinal bending. This type of bending can occur if a surface loading such as a vehicular loading or an embankment loading is applied to the soil above the pipe or culvert.

Fourier transforms are used to reduce the three-dimensional problem to one involving only two spatial directions, thereby reducing the data preparation and computation time. Conventional finite element analysis is used to approximate the field quantities in the transformed two-dimensional plane. Two Fourier integral element types have been developed which have many applications in geotechnical engineering.

KEY WORDS: elasticity; buried pipes; surface loading; soil–structure interaction

INTRODUCTION

Many problems that face engineers are three-dimensional in nature but can be simplified into a two-dimensional analysis. One of the areas where this can be done is in the analysis of long span culverts, arches and tunnels where the soil profile and the buried structure are similar in one or more co-ordinate directions. For strip loadings, a conventional plane strain analysis could be undertaken. However, vehicle loading induces a three-dimensional stress pattern, especially on shallow buried structures.

To approximate the loading for such problems, an analytical elastic solution such as the Boussinesq solution for a vertical load at the surface of an elastic half-space may be used to convert the three-dimensional loading to an equivalent line load which can be examined using conventional two-dimensional finite element analysis. This approach, however, disregards the interaction between the structure and the surrounding soil. Ideally, a three-dimensional finite element analysis could be used to analyse the problem.

Although a lot of research has been carried out into the transverse behaviour of pipes and culvert sections (e.g. see References 1–3 and 21) the three-dimensional nature of the loading has prevented similar examination of the longitudinal deformation and bending. Accurate three-dimensional finite element analysis (e.g. see Reference 4) is extremely time consuming and prone to undetected errors.

Poulos⁵ presented a method of analysis which could be used for predicting the behaviour of pipelines buried in a soil layer and subjected to a surface loading. This involved treating the pipe as a thin horizontal flexible strip of finite length pinned at the ends. Selvadurai⁶ has presented results for longitudinal moments in pipeline groups subject to a point load such as would be applied by an anchor designed to hold down pipes under hydrostatic uplift pressures. O'Rourke and Ahmed⁷ have carried out a three-dimensional finite element analysis of pipelines subjected to

vehicle loadings. Selvadurai and Pang⁸ carried out an analysis of buried pipes subjected to discontinuous displacement such as would occur due to faulting. A more recent paper by Selvadurai and Shinde⁹ presents some results for longitudinal moments in buried pipes due to a surface patch load, but does not include predictions of in-plane forces and moments. Moore^{2,3} presented a semi-analytical procedure to estimate the response of buried tubes to surface loads. His solution was based on infinitely long line loads. Takagi¹⁰ looked at the problem of longitudinal bending strain of pipelines subjected to vehicle loads. He analysed the problem using the theory for a beam on an elastic foundation.

All these approaches involve disadvantages. The finite element methods used require the generation of three-dimensional finite element meshes and the solution of large sets of equations, while Poulos' method involves the analysis of a section of the pipeline and making some assumptions about the boundary conditions at the ends of the pipe. Also the methods of Poulos and Tagaki only give longitudinal moments; they are not able to model the transverse moments and forces in the pipeline.

Small and Wong¹¹ used an integral transform technique to analyse these types of three-dimensional problems. In problems where the soil profile is constant in one co-ordinate direction, a Fourier series can be used to represent the field quantities in that direction, simplifying the problem from three dimensions to two. In general, this type of analysis has been termed the finite strip or finite prism method. Small and Wong extended the finite strip method to elastic continuum elements which are applicable to geotechnical problems. Their method relied upon the use of finite element techniques to approximate the transform field quantities in a plane containing two of the co-ordinate axes.

Small and Ngu,¹² using the method described in the earlier paper by Small and Wong, looked at the problem of longitudinal bending in pipelines subjected to embankment loading. They modelled the pipeline cross-section as a solid section with the same cross-sectional area and bending stiffness as the actual pipeline. This assumption meant that the longitudinal bending of the pipeline would be modelled correctly but it was not possible to get the correct transverse moments and stresses.

Moore and Brachman¹³ used the method of Small *et al.* to look at the hoop thrust distribution of flexible circular culverts under vehicle loading. They modelled the transverse behaviour of the pipeline. However, at shallow depths, transverse and longitudinal bending plays a far more significant role than the hoop thrust and the type of element used in their analysis cannot model this behaviour directly.

This paper extends the method of Small and Wong¹¹ to infinitely long plate elements. This allows modelling of problems such as the behaviour of flexible culverts at shallow depths under vehicular loading. The transverse behaviour of the culvert can be examined using the infinitely long plate elements (extension of the finite strip method) while the surrounding soil is modelled using the Fourier transform continuum elements developed by Small and Wong. This enables direct calculation of shear, axial forces and moments (both longitudinal and transverse) for the culvert.

IDEALIZATION

It is assumed that the soil will behave as an elastic continuum with no plastic failure. Given that in practice, the soil surrounding the culvert is usually well compacted prior to vehicular loading, this is a reasonable assumption. It is also assumed that there is no slip between the plate elements (culvert) and the adjacent continuum elements (soil) when deformation occurs and that there is no movement of the soil past the culvert. This assumption is also generally true in practice as the culvert tends to settle with the soil unless the soil is very soft relative to the pipe.

All field quantities and the three-dimensional loading are transformed (in the z direction) by the use of a Fourier transform. It is assumed that the global z co-ordinate is aligned parallel to the longitudinal axis of the pipeline or culvert. A two-dimensional finite element mesh is used to model the transformed displacement field in the x - y plane. To evaluate the response in the z direction, the Fourier transform is inverted to determine the actual displacements and stresses. Numerical integration of the transformed field quantities is used to determine values such as displacements and stress in the real x - y - z space. Direct output of bending moments (both longitudinal and transverse), shears and axial forces for the culvert is obtained.

BASIC EQUATIONS

For a general non-homogeneous anisotropic material, the governing equations may be written as follows:

(i) *The equation of equilibrium*

Static equilibrium in the body is expressed as:

$$\sigma_{kl,i} = F_k \quad (1)$$

where the vector σ denotes total stress increases and the vector F denotes body force increases (force per unit volume). The summation convention for repeated indices applies: a comma denotes partial differentiation, and indices vary over the set x, y, z .

(ii) *The strain-displacement relationships*

The strain components are related to the displacements by the usual set of relations, i.e.

$$\varepsilon_{kl} = \frac{1}{2}(u_{k,i} + u_{i,k}) \quad (2)$$

where u_k are the components of displacement.

(iii) *The stress-strain relationship*

The changes in the stress components are related to the strain components by

$$\sigma_{jk} = R_{jklm} \varepsilon_{lm} \quad (3)$$

where ε_{lm} are the components of strain, and R_{jklm} are the elastic coefficients relating stress to strain for a general anisotropic stress-strain law.

BOUNDARY CONDITIONS

The above equations must be solved subject to the boundary conditions:

$$\begin{aligned} \sigma_{jk} n_j &= T_j \quad \text{on } S_T \\ u_j &= 0 \quad \text{on } S_D \end{aligned} \quad (4)$$

where n_j are the direction cosines of the outward normal to the surface S_T which is subjected to surface traction T_j . The surface S_D has prescribed displacement boundary conditions which will

be zero for a fixed boundary. S_T and S_D make up the entire surface of the body under consideration.

FOURIER TRANSFORMS

To simplify the governing equations of the preceding section, a Fourier transform (e.g. see Reference 14) may be applied to the field quantities. In applying such a transform, the assumption is made that the properties of the soil and structure do not change in the z direction (see Figure 1) although they may change in the x - y plane. Suppose that a vertical loading, symmetric about $z = 0$, is applied to the surface of a layer as shown in Figure 1. In this case, the displacements in the x and y directions (u_x and u_y) and the in-plane rotation (of a plate) about the z axis (θ) would be symmetric along the z axis, while the displacements in the z direction (u_z) would be anti-symmetric along the z axis. Hence u_x , u_y and θ are even functions of z , while u_z is an odd function of z and these can be represented by the following transforms.

$$U_x = \frac{1}{2\pi} \int_{-\infty}^{+\infty} u_x \cos \alpha z \, dz, \quad U_y = \frac{1}{2\pi} \int_{-\infty}^{+\infty} u_y \cos \alpha z \, dz, \quad U_z = \frac{1}{2\pi} \int_{-\infty}^{+\infty} u_z \sin \alpha z \, dz, \quad (5)$$

$$\Theta = \frac{1}{2\pi} \int_{-\infty}^{+\infty} \theta \cos \alpha z \, dz$$

The equivalent inverse transforms take the form:

$$u_x = \int_{-\infty}^{+\infty} U_x \cos \alpha z \, d\alpha, \quad u_y = \int_{-\infty}^{+\infty} U_y \cos \alpha z \, d\alpha, \quad u_z = \int_{-\infty}^{+\infty} U_z \sin \alpha z \, d\alpha, \quad (6)$$

$$\theta = \int_{-\infty}^{+\infty} \Theta \cos \alpha z \, d\alpha$$

The transform of the vertical loading takes the form:

$$T_y = \frac{1}{2\pi} \int_{-\infty}^{+\infty} t_y \cos \alpha z \, dz \quad (7)$$

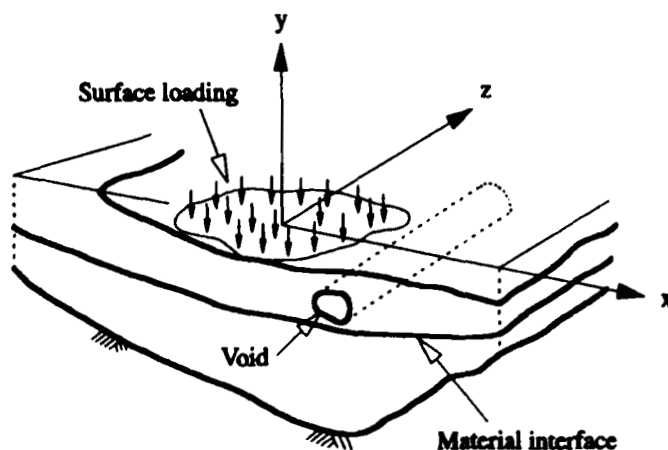


Figure 1. Typical problem

with the equivalent inverse transform

$$t_y = \int_{-\infty}^{+\infty} T_y \cos \alpha z \, d\alpha \quad (8)$$

VIRTUAL WORK FORMULATION

The finite element method can be derived by making use of the usual equations of virtual work (e.g. see Reference 4). Equations (1) to (4) are satisfied if:

$$\int_V d\epsilon^T \sigma \, dV = \int_S u^T t \, dS \quad (9)$$

Instead of substituting, say,

$$u_x = \int_{-\infty}^{+\infty} U_x \cos \alpha z \, d\alpha \quad (10)$$

to represent the displacement in the x direction, only the integrand

$$u_{ix} = U_x \cos \alpha z \quad (11)$$

is required, as long as all the other field quantities are also substituted by their integrands. These quantities will satisfy the transformed governing equations and boundary conditions. Substituting the integrands into equation (9) results in

$$\int_V d\epsilon_1^T \sigma_1 \, dV = \int_S u_1^T t_1 \, dS \quad (12)$$

For example, for a continuum element;

$$u_1 = \begin{pmatrix} U_x \cos \alpha z \\ U_y \cos \alpha z \\ U_z \sin \alpha z \end{pmatrix} \quad (13a)$$

and for a plate element,

$$u_1 = \begin{pmatrix} U_x \cos \alpha z \\ U_y \cos \alpha z \\ U_z \sin \alpha z \\ \Theta \cos \alpha z \end{pmatrix} \quad (13b)$$

FINITE ELEMENT APPROXIMATION

The transformed field variables may be approximated in the usual finite element fashion. The general equation is given by:

$$U_1 = N \Delta_m \quad (14)$$

where U_1 is the vector of transformed displacements, N the matrix of shape or interpolating functions, Δ_m is the vector of the nodal values of U_1 for element m . The form of the matrix N depends on the element type adopted. The discretization is carried out in the x - y plane using plate elements for the culvert and continuum elements for the surrounding soil, as shown in Figure 2.

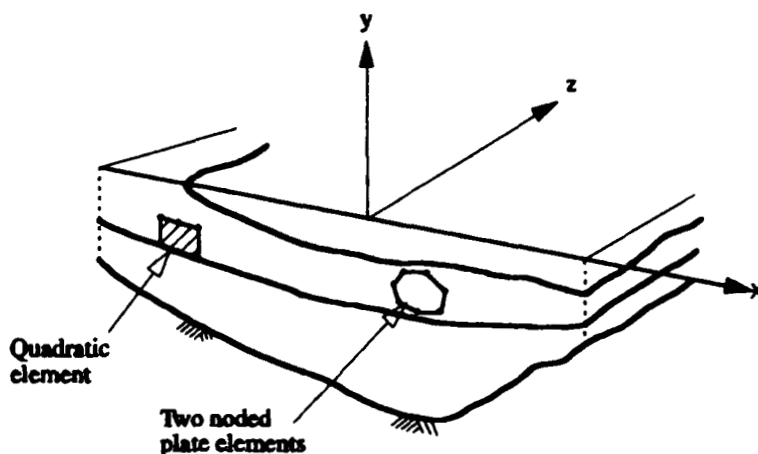


Figure 2. Finite element representation of the typical problem

The transformed strain components are computed from the displacements in the standard way, i.e.

$$\epsilon_1 = \mathbf{B}\Delta_m \quad (15)$$

where ϵ_1 is the vector of transformed strain components and \mathbf{B} is the matrix relating transformed strains to transformed nodal displacements.

We may also write the stress-strain relationship as

$$\sigma_1 = \mathbf{D}\epsilon_1 \quad (16)$$

where \mathbf{D} is the matrix of elastic constants relating stress to strain. Substitution of (14), (15) and (16) into equation (12) leads to a set of transformed stiffness equations

$$d\Delta^T \left(\sum_{m=1}^M \int_{V_m} \mathbf{B}^T \mathbf{D} \mathbf{B} dV_m \right) \Delta = d\Delta^T \left(\sum_{m=1}^M \int_{S_m} \mathbf{N}^T \mathbf{T} dS_m \right) \quad (17)$$

where Δ is the vector of the transformed displacements for the entire system and M is the number of elements.

Since $d\Delta$ are arbitrary variations which are not necessarily zero, equation (17) becomes

$$\mathbf{K}\Delta = \mathbf{F} \quad (18)$$

where \mathbf{K} and \mathbf{F} are the global 'stiffness matrix' and 'load vector' assembled from the appropriate element matrices \mathbf{K}_m and \mathbf{F}_m , and

$$\mathbf{K}_m = \int_{A_m} (\bar{\mathbf{B}}^T \mathbf{D} \bar{\mathbf{B}}) dA_m \quad (19)$$

$$\mathbf{F}_m = \int_{\Gamma_m} (\mathbf{N}^T \mathbf{T}) d\Gamma_m \quad (20)$$

A_m is the area of element m and Γ_m is the length of the loaded surface. (The above matrices are expanded in full in Appendix A).

Numerical integration is necessary for the evaluation of the stiffness matrices \mathbf{K}_m in equation (19) since the matrix \mathbf{B} contains functions of both x and y . The solution of equation (18) will provide values of the transformed displacements at the nodes Δ . The actual displacements \mathbf{u} are obtained by inverting the transformed values (see equation (6)). The infinite integral is truncated to some large finite value and evaluated using Gaussian quadrature.

For an even function such as u_x , the integral is approximated by

$$u_x = \sum_{j=1}^N W_j U_x(\alpha_j) \cos \alpha_j z \quad (21)$$

where W_j are the Gaussian weights and the α_j are the Gaussian co-ordinates. Hence equation (18) is solved for a particular value of α_j to obtain U_x , and these are then summed to get the actual field values as shown in equation (21).

VALIDATION OF THE ALGORITHM

The above equations were incorporated into a general finite element program, AFENA.¹⁵ AFENA was then tested against analytical solutions and other programs to validate the formulation.

The continuum elements were tested against Holl's solution¹⁶ reproduced in the text 'Elastic Solutions for Soil and Rock Mechanics' by Poulos and Davis.¹⁷ This solution determines the distribution of stresses beneath the corner of a uniformly loaded rectangle. 196 eight noded elastic continuum elements, each with 9 Gauss points were used in the finite element analysis. They were assigned the following properties:

$$E = 10,000 \text{ kPa}$$

$$\nu = 0.3$$

$$q = 100 \text{ kPa over a } 2 \text{ m} \times 2 \text{ m square patch on the surface}$$

where E and ν are the Young's modulus and Poissons ratio of the elastic continuum and q is the intensity of the vertical surface loading.

The finite element mesh used in the analysis is shown in Figure 3. Symmetry was used to reduce the dimensions of the problem: the left-hand boundary was treated as the centreline of the loaded area. The other boundaries were assumed to be rigid and 'smooth'.

A comparison between the analytical solution and the results of the finite element program is shown in Figure 4. The comparison demonstrates that the finite element program is successfully able to model a three-dimensional problem using Fourier transforms in the z direction and finite elements in the x - y plane.

To test the plate elements, two sets of tests were carried out. The first set of tests was against a plane strain problem. This involved a strip load on the surface of the soil, above a long culvert. The soil was modelled using 8-noded continuum elements while the culvert was modelled using 2-noded plate elements. The mesh used in AFENA is shown in Figure 5. Once again, symmetry was used to reduce the problem size. The right-hand boundary was treated as the centreline of the loaded area. The other boundaries were assumed to be rigid and 'smooth'.

Two analyses were carried out using the mesh shown in Figure 5. One was a conventional plane strain analysis while the other used the Fourier integral elements. To approximate the plane strain solution, a long surface load was modelled using the Fourier transform technique.

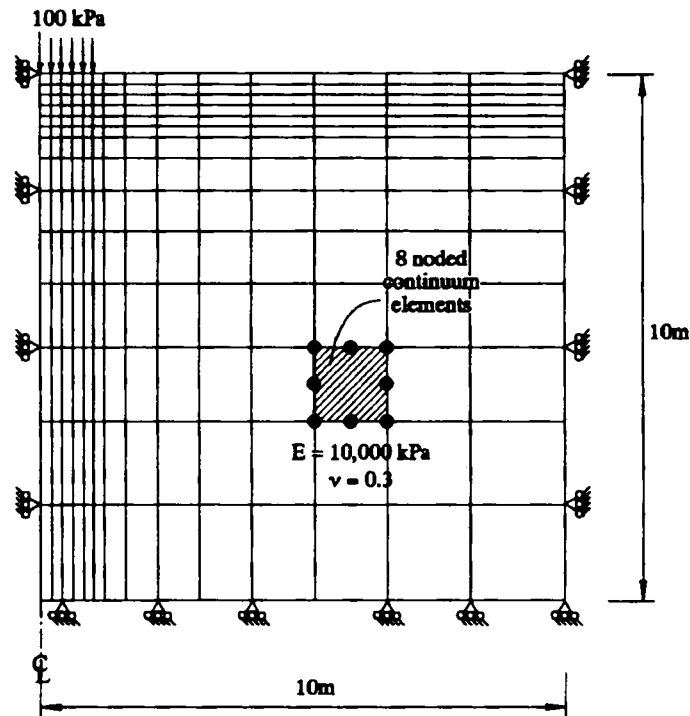


Figure 3. Finite element mesh used in the Holl problem

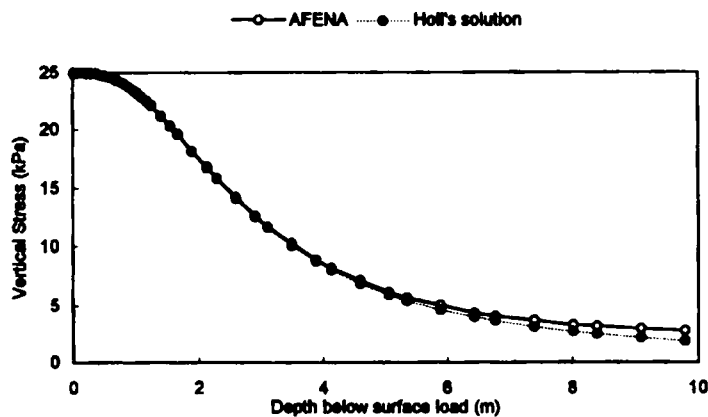


Figure 4. Comparison of numerical and analytical solutions for vertical stresses beneath the corner of a rectangular load

The solutions obtained using the plane strain analysis and the approximation to plane strain using the Fourier integral elements were compared. The transverse moments in the pipeline predicted by both analyses are shown in Figure 6. Again there is good agreement between the results.

In the second set of tests, the plate elements were tested against an independent program, FEAR.¹⁸ This program calculates moments in rafts due to patch loads. The raft is modelled using

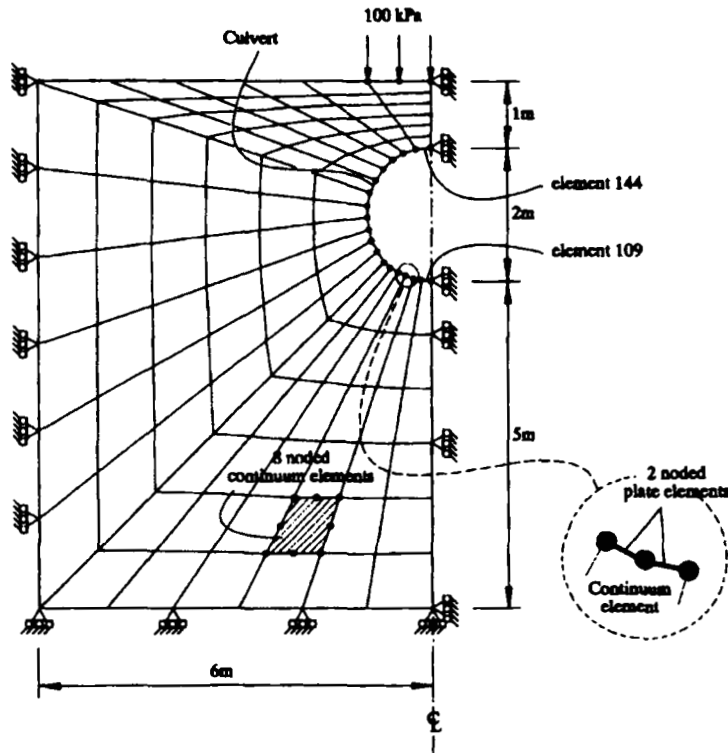


Figure 5. Finite element model of a buried pipe

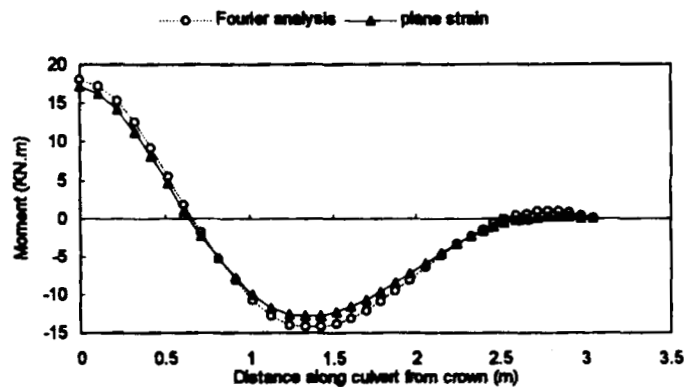


Figure 6. Comparison of numerical solutions for strip loading above a buried pipe

finite elements while the soil below is modelled using an analytical solution for a loading on the surface of an elastic half space. The soil is assumed to be uniformly elastic and infinitely deep. The interface between the raft and the soil is assumed to be smooth.

For consistency with the assumptions of the program FEAR, a raft on a deep layer of soil was modelled with a uniform vertical pressure applied over a rectangular patch in the centre of the

raft. Figure 7 shows a schematic diagram of the problem analysed and the finite element mesh used is shown in Figure 8. Symmetry was used to reduce the problem size with the right-hand boundary corresponding to the centreline of the loaded area. The other boundaries were assumed to be rigid and smooth. The following properties were assumed for the soil and the raft:

RAFT

$$E = 1000 \text{ kPa}, \quad \nu = 0.3, \quad t = 0.5 \text{ m}, \quad L = 22 \text{ m}, \quad W = 4 \text{ m}$$

where L , W and t are the length, width and thickness of the raft, respectively.

SOIL

$$E = 50 \text{ kPa}, \quad \nu = 0.49 (\sim 0.5)$$

LOAD

$$q = 100 \text{ kPa over a } 2 \text{ m} \times 2 \text{ m square patch on the surface}$$

These quantities are not intended to be realistic. They have been chosen merely to provide a basis for comparison of the two different solutions.

FEAR assumes a smooth interface between the raft and the soil, whereas AFENA assumes a rough interface. As a result, the Poisson's ratio of the soil was assumed to be approximately 0.5. Theoretically, this should give the same solution for both rough and smooth interfaces. In FEAR, the raft is assigned a finite length (22 m), but it has a relatively large aspect ratio ($22/4 = 5.5$), so that over most of its length it will behave as if it had infinite length. Of course, in the Fourier transform analysis, the raft is actually of infinite length.

The moments in the raft along the centerline in both the x and z direction are shown in Figure 9 while the in-plane rotations and the vertical displacements are shown in Figure 10. Given the relatively coarse finite element mesh, there is very good agreement between the two independent solutions. Once again, the ability to predict moments in both the transverse and longitudinal directions is demonstrated.

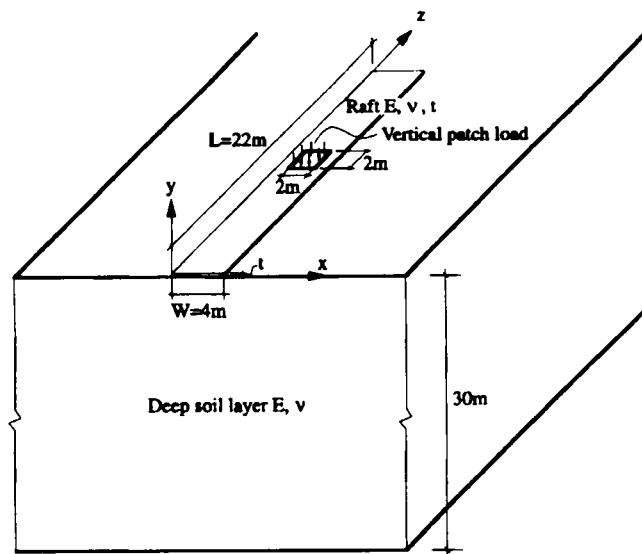


Figure 7. Definition of the raft loading problem

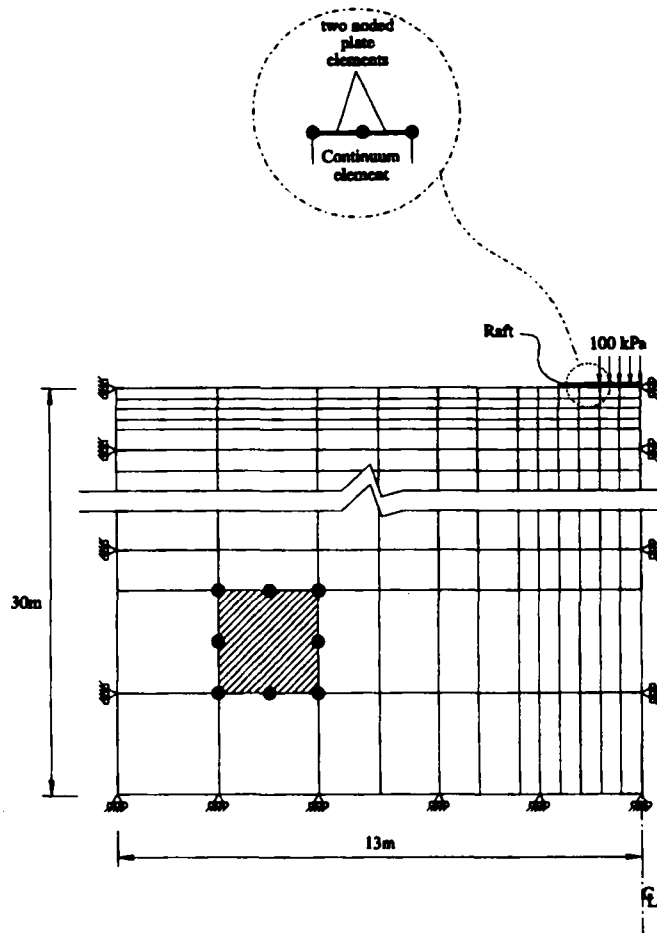


Figure 8. Finite element model of a raft on elastic soil

SUMMARY AND CONCLUSIONS

The Fourier transform method of Small and Wong¹¹ has been extended to include plate elements that allow direct calculation of moments, deflections and strains in buried structures such as pipelines, arches and culverts.

The method involves the application of a Fourier transform to the field variables thereby reducing the problem to one involving two spatial dimensions. The inverse transform is applied to find the solution at any co-ordinate position in three dimensions. Generally, Gaussian integration is used to carry out the inverse transformation.

The program has been tested against various analytical solutions and other independent techniques to confirm its validity. The method is valid in cases where the soil can be idealized as an elastic material. Parametric studies on the behaviour of arches, box culverts and pipelines are currently being carried out and will be the subject of future papers. These will include predictions of bending moments, axial forces and displacements.

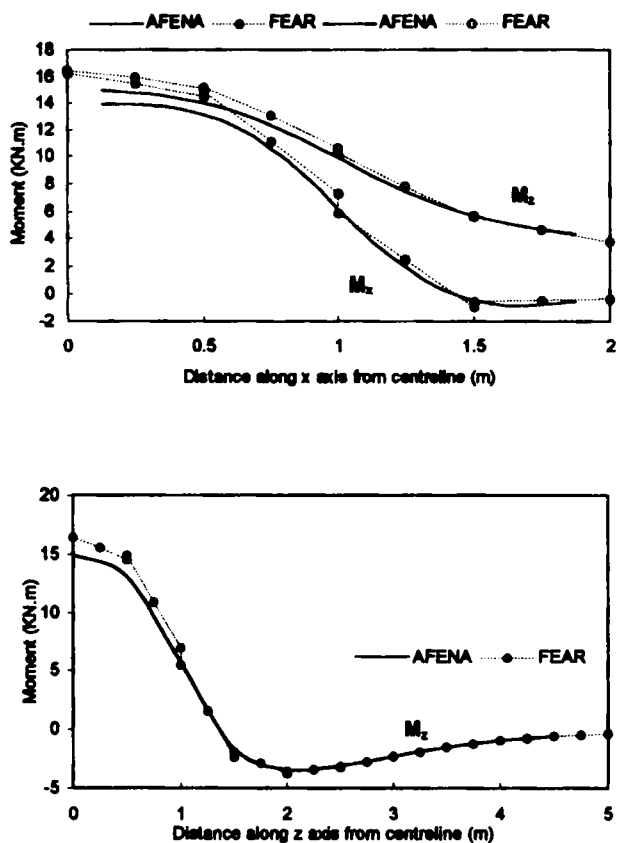


Figure 9. Comparison of numerical solutions for bending moments in the raft

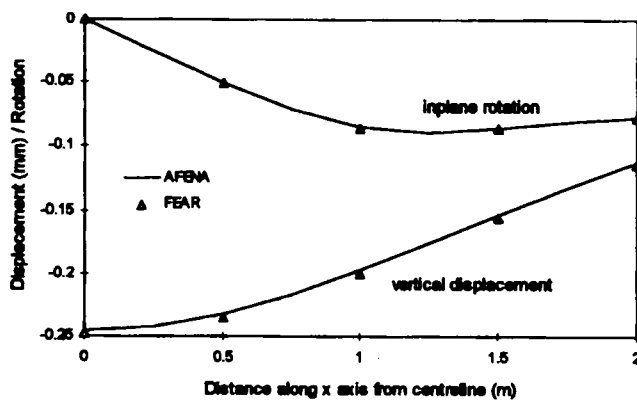


Figure 10. Comparison of numerical solutions for vertical displacement and rotation

APPENDIX

The transformed displacements can be represented as

$$\mathbf{u}_1 = \begin{Bmatrix} U_x \cos \alpha z \\ U_y \cos \alpha z \\ U_z \sin \alpha z \end{Bmatrix} \quad (22)$$

Suppose that we can express the transformed displacement within an element having n nodes in terms of interpolating functions $N_1, N_2, N_3, \dots, N_n$. We may then write

$$\mathbf{u}_1 = \mathbf{N} \Delta_m \quad (23)$$

where Δ_m is the vector of nodal values of the transformed displacements for element m .

Continuum elements

For the continuum elements, we have:

$$\Delta_m = (U_{x1}, U_{y1}, U_{z1}, U_{x2}, U_{y2}, U_{z2}, \dots, U_{xn}, U_{yn}, U_{zn})^T \quad (24)$$

and

$$\mathbf{N} = \begin{bmatrix} N_1.c & 0 & 0 & N_2.c & 0 & 0 & \dots & N_n.c & 0 & 0 \\ 0 & N_1.c & 0 & 0 & N_2.c & 0 & \dots & 0 & N_n.c & 0 \\ 0 & 0 & N_1.s & 0 & 0 & N_2.s & \dots & 0 & 0 & N_n.s \end{bmatrix} \quad (25)$$

with the shape functions being dependant on the type of interpolation polynomial chosen and where

$$c = \cos \alpha z, \quad s = \sin \alpha z$$

The strain components, which include engineering shear strains, are computed from the displacements in the usual way using

$$\boldsymbol{\varepsilon} = \begin{Bmatrix} \varepsilon_{xx} \\ \varepsilon_{yy} \\ \varepsilon_{zz} \\ \gamma_{xy} \\ \gamma_{yz} \\ \gamma_{zx} \end{Bmatrix} = \begin{bmatrix} \frac{\partial u_x}{\partial x} \\ \frac{\partial u_y}{\partial y} \\ \frac{\partial u_z}{\partial z} \\ \frac{\partial u_x}{\partial y} + \frac{\partial u_y}{\partial x} \\ \frac{\partial u_y}{\partial z} + \frac{\partial u_z}{\partial y} \\ \frac{\partial u_x}{\partial z} + \frac{\partial u_z}{\partial x} \end{bmatrix} \quad (26)$$

so that

$$\boldsymbol{\varepsilon}_1 = \mathbf{B} \Delta_m \quad (27)$$

where

$$\mathbf{B} = [\mathbf{B}_1, \mathbf{B}_2, \mathbf{B}_3, \dots, \mathbf{B}_j, \dots, \mathbf{B}_n] \quad (28)$$

and

$$\mathbf{B}_j = \begin{bmatrix} \frac{\partial N_j}{\partial x} \cos \alpha z & 0 & 0 \\ 0 & \frac{\partial N_j}{\partial y} \cos \alpha z & 0 \\ 0 & 0 & \alpha N_j \cos \alpha z \\ \frac{\partial N_j}{\partial y} \cos \alpha z & \frac{\partial N_j}{\partial x} \cos \alpha z & 0 \\ 0 & -\alpha N_j \sin \alpha z & \frac{\partial N_j}{\partial y} \sin \alpha z \\ -\alpha N_j \sin \alpha z & 0 & \frac{\partial N_j}{\partial x} \sin \alpha z \end{bmatrix} \quad (29)$$

The relationship between stress and strain can be written as follows

$$\boldsymbol{\sigma}_1 = \begin{Bmatrix} \sigma_{xx} \\ \sigma_{yy} \\ \sigma_{zz} \\ \tau_{xy} \\ \tau_{yz} \\ \tau_{zx} \end{Bmatrix} = \mathbf{D} \boldsymbol{\epsilon}_1 \quad (30)$$

where \mathbf{D} is the matrix of elastic constants relating stress to strain.

Two noded plate elements

The nodal degrees of freedom for a plate element are:

$$\Delta_m = (U_{x1}, U_{y1}, U_{z1}, \Theta_1, U_{x2}, U_{y2}, U_{z2}, \Theta_2)^T \quad (31)$$

and

$$\mathbf{N} = \begin{bmatrix} N_{11}.c & 0 & 0 & 0 & N_{21}.c & 0 & 0 & 0 \\ 0 & N_{12}.c & 0 & N_{13}.c & 0 & N_{22}.c & 0 & N_{23}.c \\ 0 & 0 & N_{11}.s & 0 & 0 & 0 & N_{21}.s & 0 \end{bmatrix} \quad (32)$$

where

$$c = \cos \alpha z, \quad s = \sin \alpha z$$

Specific forms of the interpolation functions may be found in texts on the finite strip method.^{19,20}

The components of 'strain' in the plate are computed from the displacements using

$$\epsilon = \begin{Bmatrix} \epsilon_{xx} \\ \epsilon_{zz} \\ \gamma_{xz} \\ -\chi_x \\ -\chi_z \\ 2\chi_{xz} \end{Bmatrix} = \begin{Bmatrix} \frac{\partial u_x}{\partial x} \\ \frac{\partial u_z}{\partial z} \\ \frac{\partial u_x}{\partial z} + \frac{\partial u_z}{\partial x} \\ -\frac{\partial^2 u_y}{\partial x^2} \\ -\frac{\partial^2 u_y}{\partial z^2} \\ 2\frac{\partial^2 u_y}{\partial x \partial z} \end{Bmatrix} \quad (33)$$

where

$$\epsilon_1 = \mathbf{B} \Delta_m \quad (34)$$

$$\mathbf{B} = [\mathbf{B}_1, \mathbf{B}_2] \quad (35)$$

and

$$\mathbf{B} = \begin{bmatrix} \frac{\partial N_{11}}{\partial x} \cos \alpha z & 0 & 0 & 0 \\ 0 & 0 & \alpha N_{11} \cos \alpha z & 0 \\ -\alpha N_{11} \sin \alpha z & 0 & \frac{\partial N_{11}}{\partial x} \sin \alpha z & 0 \\ 0 & -\frac{\partial^2 N_{12}}{\partial x^2} \cos \alpha z & 0 & -\frac{\partial^2 N_{13}}{\partial x^2} \cos \alpha z \\ 0 & \alpha^2 N_{12} \cos \alpha z & 0 & \alpha^2 N_{13} \cos \alpha z \\ 0 & -2\alpha \frac{\partial N_{12}}{\partial x} \sin \alpha z & 0 & -2\alpha \frac{\partial N_{13}}{\partial x} \sin \alpha z \end{bmatrix} \text{ etc.}$$

The relationship between 'stress' and 'strain' in the plate can be written as follows

$$\sigma_1 = \begin{Bmatrix} \sigma_x \\ \sigma_z \\ \tau_{xz} \\ M_x \\ M_z \\ M_{xz} \end{Bmatrix} = \mathbf{D} \epsilon_1 \quad (36)$$

where \mathbf{D} is the matrix of appropriate elastic constants.

Solution of equations

The **B** matrices shown above contain both sine and cosine terms. For example, the **B** matrix for node *j* of the continuum elements is

$$\mathbf{B}_j = \begin{bmatrix} \frac{\partial N_j}{\partial x} \cos \alpha z & 0 & 0 \\ 0 & \frac{\partial N_j}{\partial y} \cos \alpha z & 0 \\ 0 & 0 & \alpha N_j \cos \alpha z \\ \frac{\partial N_j}{\partial y} \cos \alpha z & \frac{\partial N_j}{\partial x} \cos \alpha z & 0 \\ 0 & -\alpha N_j \sin \alpha z & \frac{\partial N_j}{\partial y} \sin \alpha z \\ -\alpha N_j \sin \alpha z & 0 & \frac{\partial N_j}{\partial x} \sin \alpha z \end{bmatrix} \quad (37)$$

This can be separated into two parts as follows

$$\mathbf{B}_j = {}^c\mathbf{B}_j \cos \alpha z + {}^s\mathbf{B}_j \sin \alpha z \quad (38)$$

where

$${}^c\mathbf{B}_j = \begin{bmatrix} \frac{\partial N_j}{\partial x} & 0 & 0 \\ 0 & \frac{\partial N_j}{\partial y} & 0 \\ 0 & 0 & \alpha N_j \\ \frac{\partial N_j}{\partial y} & \frac{\partial N_j}{\partial x} & 0 \\ 0 & 0 & 0 \\ 0 & 0 & 0 \end{bmatrix}, \quad {}^s\mathbf{B}_j = \begin{bmatrix} 0 & 0 & 0 \\ 0 & 0 & 0 \\ 0 & 0 & 0 \\ 0 & 0 & 0 \\ 0 & -\alpha N_j & \frac{\partial N_j}{\partial y} \\ -\alpha N_j & 0 & \frac{\partial N_j}{\partial x} \end{bmatrix} \quad (39)$$

The matrix \mathbf{K}_m now becomes

$$\begin{aligned} \mathbf{K}_m &= \int_{V_m} ({}^c\mathbf{B} \cos \alpha z + {}^s\mathbf{B} \sin \alpha z)^T \mathbf{D} ({}^c\mathbf{B} \cos \alpha z + {}^s\mathbf{B} \sin \alpha z) dV \\ &= \int_{V_m} {}^c\mathbf{B}^T \mathbf{D} {}^c\mathbf{B} \cos^2 \alpha z dV + \int_{V_m} {}^s\mathbf{B}^T \mathbf{D} {}^s\mathbf{B} \sin^2 \alpha z dV \end{aligned} \quad (40)$$

The integration over the volume lies between $\pm \infty$ in the *z* direction and over finite dimensions in the *x*-*y* plane. Because $\int_{-\infty}^{+\infty} \cos \alpha z \sin \alpha z dz = 0$, it is not necessary to retain these terms in the stiffness matrix.

If element m is loaded by tractions which are even functions of z , the force vector F_m may be written according to equation (17) as

$$F_m = \int_{S_m} N^T T \cos^2 \alpha z \, dS_m \quad (41)$$

Equation (17) now becomes

$$\sum_{m=1}^M \left(\int_{V_m} {}^c \mathbf{B}^T \mathbf{D} {}^c \mathbf{B} \cos^2 \alpha z \, dV_m + \int_{V_m} {}^s \mathbf{B}^T \mathbf{D} {}^s \mathbf{B} \sin^2 \alpha z \, dV_m \right) \Delta = \sum_{m=1}^M \int_{S_m} N^T T \cos^2 \alpha z \, dS_m \quad (42)$$

Because the integral over the volume V_m and surface area S_m includes an integration in the z direction from $\pm \infty$, and since

$$\int_{-\infty}^{+\infty} \cos^2 \alpha z \, dz = \int_{-\infty}^{+\infty} \sin^2 \alpha z \, dz \quad (43)$$

cancelling $\int_{-\infty}^{+\infty} \cos^2 \alpha z \, dz$ and $\int_{-\infty}^{+\infty} \sin^2 \alpha z \, dz$ from both sides of equation (4) results in

$$\mathbf{K} \Delta = \mathbf{F} \quad (44)$$

where \mathbf{K} and \mathbf{F} are the global 'stiffness matrix' and load vector assembled from the appropriate element matrices \mathbf{K}_m and \mathbf{F}_m , where

$$\mathbf{K}_m = \int_{A_m} ({}^c \mathbf{B}^T \mathbf{D} {}^c \mathbf{B} + {}^s \mathbf{B}^T \mathbf{D} {}^s \mathbf{B}) \, dA_m \quad (45)$$

$$\mathbf{F}_m = \int_{\Gamma_m} (N^T T) \, d\Gamma_m \quad (46)$$

A_m is the area of element m and Γ_m is the length of the loaded surface.

Now

$${}^c \mathbf{B}^T \mathbf{D} {}^s \mathbf{B} = {}^s \mathbf{B}^T \mathbf{D} {}^c \mathbf{B} = 0,$$

so that

$${}^c \mathbf{B}^T \mathbf{D} {}^c \mathbf{B} + {}^s \mathbf{B}^T \mathbf{D} {}^s \mathbf{B} = \mathbf{B}^T \mathbf{D} \mathbf{B} \quad (47)$$

Hence equation (46) becomes

$$\mathbf{K}_m = \int_{A_m} (\mathbf{B}^T \mathbf{D} \mathbf{B}) \, dA_m \quad (48)$$

where

$$\mathbf{B} = [\mathbf{B}_1, \mathbf{B}_2, \mathbf{B}_3, \dots, \mathbf{B}_j, \dots, \mathbf{B}_n]$$

and

$$\mathbf{B}_j = \begin{bmatrix} \frac{\partial N_j}{\partial x} & 0 & 0 \\ 0 & \frac{\partial N_j}{\partial y} & 0 \\ 0 & 0 & \alpha N_j \\ \frac{\partial N_j}{\partial y} & \frac{\partial N_j}{\partial x} & 0 \\ 0 & -\alpha N_j & \frac{\partial N_j}{\partial y} \\ -\alpha N_j & 0 & \frac{\partial N_j}{\partial x} \end{bmatrix} \quad (49)$$

for the continuum elements.

i.e.

$$\mathbf{B}_j = {}^c\mathbf{B}_j + {}^s\mathbf{B}_j$$

A similar result is obtained for the plate elements. As a result, the matrix \mathbf{B} in the stiffness formulation (equation 17) is evaluated without the sine and cosine terms. However, when evaluating the stresses from the displacements, the full \mathbf{B} matrix containing the sine and cosine terms must be used.

REFERENCES

1. I. D. Moore, Buckling of Buried Flexible Structures of Noncircular Shape, in G. Swoboda, (ed.), *Proc. 6th Int. Conf. Numer. Methods in Geomechanics, Innsbruck*, 2, 1079–1084, Balkema, Rotterdam (1988).
2. I. D. Moore, The elastic stability of shallow buried tubes *Géotechnique*, 37(2), 151–161 (1987).
3. I. D. Moore, Response of Buried Cylinders to Surface Loads *J. Geotech. Eng. ASCE* 113(7), 758–773 (1987).
4. O. C. Zienkiewicz and R. L. Taylor, *The Finite Element Method*, McGraw Hill Book Company, London, 1977.
5. H. G. Poulos, Analysis of longitudinal behaviour of pipes, *Proc. Conf. on Analysis and Design in Geotech. Eng.*, 1, University of Texas, Austin, ASCE Publication 1974, pp. 198–223.
6. A. P. S. Selvadurai, A soil-structure interaction problem for a group of connected flexible pipelines, in M. B. Pickell, (ed.), *Proc. Conf. on Pipelines in Adverse Environments II*, ASCE, 1983.
7. T. D. O'Rourke and I. Ahmed, Effect of shallow trench construction on cast iron pipe lines, in J. K. Jeyapalan, (ed.), *Proc. Int. Conf. on Advances in Underground Pipeline Engineering*, ASCE (1985).
8. A. P. S. Selvadurai and S. Pang, Non-linear effects in soil-pipeline interaction in a ground subsidence zone, in *Proc. 6th Int. Conf. Numer. Methods in Geomechanics, Innsbruck*, 2, 1988, pp. 1085–1094, Balkema, Rotterdam.
9. A. P. S. Selvadurai and S. B. Shinde, Frost heave induced mechanics of buried pipelines, *J. Geotech. Eng., ASCE* 119, 1929–1951 (1993).
10. N. Takagi, Analysis of the longitudinal bending strain of pipelines subjected to vehicle loads, in *Proc. Symp. Undergrd. Excv. in soils and Rocks, Inc. Earth Press, Theos., Buried Struc. and Tunnels, AIT & SE Asian Geotech. Soc. Bangkok*, 1989, pp. 33–44.
11. J. C. Small and H. K. W. Wong, The use of Integral Transforms in Solving Three Dimensional Problems in Geomechanics, *Computers and Geotechnics*, 6, 199–216 (1988).
12. J. C. Small and J. T. M. Ngu, Longitudinal bending in pipelines subjected to embankment loading, in Beer, Booker and Carter, (eds), *Proc. 7th Int. Conf. Comp. Mthds. and Adv. in Geomech., Cairns*, 2, 1991, pp. 1233–1239, Balkema, Rotterdam.
13. I. D. Moore and R. W. I. Brachman, Three dimensional analysis of flexible circular culverts, *J. Geotech. Eng., ASCE* 120(10), 1829–1844 (1994).
14. I. N. Sneddon, *Fourier Transforms*, McGraw-Hill, New York, 1951.
15. J. P. Carter and N. P. Balaam, AFENA. A general finite element program for geotechnical engineering, School of Civil and Mining Engineering, University of Sydney, 1994.

16. D. L. Holl, Stress Transmission in Earths, *Proc. High. Res. Board*, **20**, 1940, pp. 709–721.
17. H. G. Poulos and E. H. Davis, *Elastic Solutions for Soil and Rock Mechanics*, Wiley, New York, 1974; Reprinted in 1991 by Centre for Geotechnical Research, University of Sydney.
18. J. C. Small, FEAR. Finite Element Analysis of Rafts, School of Civil and Mining Engineering, University, of Sydney, 1994.
19. Y. K. Cheung, *Finite Strip Method in Structural Analysis*, Pergamon Press, Oxford, 1976.
20. C. Y. Loo and A. R. Cusens, *The Finite Strip Method in Bridge Engineering*, Viewpoint, Wexham Springs, Slough, 1978.
21. R. J. Krizek, R. A. Parmelee, J. N. Kay and H. A. Elnaggar, Structural Analysis and Design of Pipe Culverts *Nat. Coop. High. Res. Prog., Rep. 116*, High. Res. Board, Washington, 1971.